

Sensor Guided Laser Welding Robot System^{*}

Chang-Hyun Kim, Tae-Yong Choi, Ju-Jang Lee^{*}
Jeong Suh, Kyoung-Taik Park, Hee-Shin Kang^{**}
Moon-Yong Lee^{***} Sung-rak Kim^{****}

^{*} Department of Electrical Engineering and Computer Science
Korea Advanced Institute of Science and Technology (KAIST)
Daejeon, Korea

(e-mail: {sunnine, ermzace}@odyssey.kaist.ac.kr, jjlee@ee.kaist.ac.kr)

^{**} Korea Institute of Machinery and Materials (KIMM)
Daejeon, Korea

(e-mail: {jsuh, ktpark, khs}@kimm.re.kr)

^{***} Technical Institute of Sungwoo Hitech Co., LTD, Korea

^{****} Hyundai Heavy Industries Co., LTD, Korea

Abstract: In order to obtain a good result in the laser welding process, the laser welding technology for manufacturing an automobile body is studied in this research. The robot, the seam tracking system, and CW Nd:YAG laser are used for the laser welding robot system. Especially, the development of the laser-stripe sensor is highlighted. The laser-stripe sensor can measure the profile of the welding object and obtain the gap and seam line. Moreover, the working distance of the sensor can be varied. The control scheme of the whole system is also presented. The profile and gap measurement and the seam tracking experiments were carried out to validate the operation of the system.

Keywords: Autonomous robotic systems; Control technology in the automotive industry; Robotics technology; Intelligent manufacturing systems; Information and sensor fusion.

1. INTRODUCTION

There is an increasing demand for the laser welding in automotive industry. Compared with the spot welding, the laser welding enables the car body to have a strong weld and light weight. Especially, the robot systems have been used in the welding manufacturing by the help of a laser source and an optical fiber. In addition, a real-time tracking is demanded in industries.

In order to obtain a good result in the welding process, the position error between the welding line and the focal point of the laser beam should be maintained below 200 μm (because the beam size at focal point is less than 500 μm). Although the welding jig fixes the car body, the seam line is distorted due to alignment and modeling errors. Therefore, the tracking technology of the seam line is needed to adjust the position of the laser welding head by detecting the exact seam line.

Many kind of sensory systems exist and the majority of available sensors make use of optical means (imaging sensors, structured or other type of light) and triangulation methods. For the welding purpose, there are several commercial devices (Forest et al. (2002)). However, the price is still high and the working distance is normally fixed according to the applications. Particularly, in case

^{*} This work is supported by the Intelligent Robot R&D Project (New Growth Engine of Korea, Ministry of Commerce, Industry and Energy).

that the seam line is not given prior or distorted in the direction of depth, the change of the working distance is needed.

The purpose of this study is to make the laser welding robot system. Especially, we focus on the development of a laser-stripe sensor for profile measurement, gap measurement and seam tracking. The sensor guided control scheme of the whole system is also presented.

This paper is organized as follows. In section 2, the laser welding robot system is described. The three dimensional robot welding system and its components are introduced. In section 3, the development of the laser-stripe sensor is represented. Both the design of the sensor and the image processing procedures are explained. The detection of the gap and seam is also given. In section 4, the sensor guided control scheme is illustrated. In section 5, some experimental results are shown. Finally, section 6 concludes this paper.

2. LASER WELDING ROBOT SYSTEM

In the welding environment, the welding seam is not straight but slightly distorted due to some difficulty resulting from the cutting the strong and thin steel plate longitudinally. And some thermal deformation can take place during welding process. Therefore, it is necessary to develop the seam tracking device and the welding apparatus to solve such problems. The robot, the seam tracking

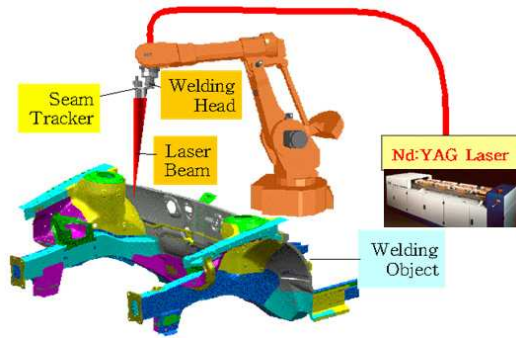


Fig. 1. Three dimensional laser welding

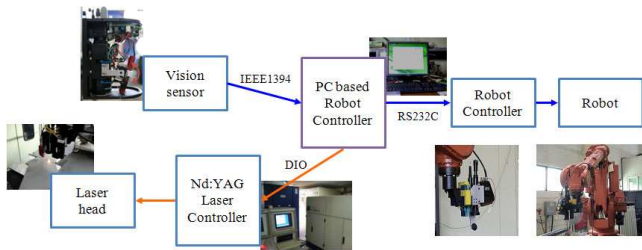


Fig. 2. Sensor guided laser welding robot system

system and CW Nd:YAG laser are used for three dimensional robot laser welding (See Fig. 1). A 4kW Nd:YAG laser and the 6 axes industrial robot are used in this study. The precise positioning ($<200 \mu m$) of the laser beam on the joint is achieved by the seam tracker. Butt and lap joints are most common welding joints of car bodies.

The seam tracking sensors can be used for teaching of seam locations prior to laser welding and for real-time tracking during laser welding. In real-time tracking applications, the sensor has to measure at least some distance ahead of the laser focal point to prevent disturbances caused by the welding process. Positional errors of the laser focal position with respect to the weld seam significantly depend on the look-ahead distance. The information about the seam line is transmitted to the main controller. Then, the corrected trajectories are generated and the motion commands are sent to the robot controller. Fig. 2 shows the total system configuration of sensor guided laser welding robot system. In this system, a newly developed laser-stripe sensor is substituted for the commercial seam tracker.

3. LASER-STRIPE SENSOR

A new laser-stripe sensor is developed. The purpose of the laser-stripe sensor is to acquire the 3 dimensional profile and seam information of the work piece from the vision sensor. In this research, a stripe-type laser diode is adopted to get the information. The sensor with the stripe-type laser diode can capture the profile image which lies within the triangular plane projected by the laser light. The 3 dimensional coordinate of the profile data can be easily calculated by triangulation. The dark-red (wavelength=660 nm) laser is used in this system and the appropriate bandpass filter is inserted in front of the lens to pass the laser light only. The configuration of the laser-stripe sensor is depicted in Fig. 3.

3.1 Mechanical & Electrical Design

The sensor consists of a PC based (IEEE1394) camera, a stripe-type laser diode, a varying focal lens, and a bandpass filter. The total system is assembled into a compact module which can be attached to the head of welding robot system. The camera can capture the 1024×768 image with the frame-rate up to 30 Hz and $10 \times$ macro zoom lens is used to get the desired accuracy.

Unlike other sensors, this sensor is designed to operate at different working distances. For this purpose, the relative angle between the camera and the laser diode can be changed. And to capture a clear and high resolution image, the zoom and the focus can be varied also. The radio controlled (RC) servo motors are adopted as actuators. The relative angle of the laser diode is crucial for the accurate measurement. The DC motor with an absolute encoder is used for the precise control of the relative angle. This enables the laser diode to be positioned at the predefined angle according to the working distance. Totally, three motors are used and the operation is fulfilled with simple links. The developed sensor is shown in Fig. 4.

3.2 Profile Measurement

The first job to get the profile is to extract the surface points from the laser line image. This process is referred as thinning or skeletonization. Thinning is an image process to find center lines from the integer valued image regions. Numerous algorithms such as row based maximum search, threshold methods, center of gravity, correlation techniques were suggested for thinning. As reported in Haug et al. (1998), the center of gravity (COG) method gives us the best accuracy among those methods.

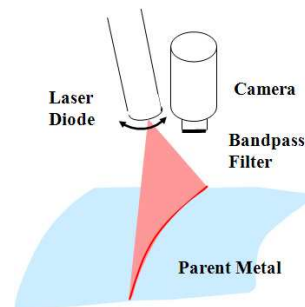


Fig. 3. Configuration of laser-stripe sensor



Fig. 4. The laser-stripe sensor

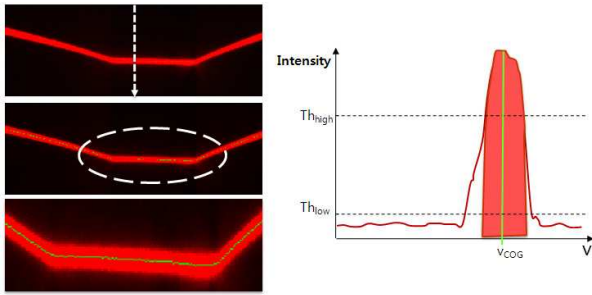


Fig. 5. Center of gravity (COG) with thresholding

Let the horizontal and vertical image coordinates be the u and v , respectively. By using COG, the center coordinate at each horizontal position is given as

$$v_{COG}(u) = \frac{\sum_v I(u, v) \times v}{\sum_v I(u, v)} \quad (1)$$

where $I(u, v)$ is the intensity of the pixel (u, v) .

In typical industrial applications where well scattering parts mix with high reflective or corroded zones, the maximum detection is needed to differentiate the main peak from others. In short, maximum detection is followed by the center of gravity around the maximum in order to extract the profile from images.

In addition, there exist small sensor noises in the entire sensing region. This makes the result of COG be independent on the peak and converge to the middle of the sensing region. To alleviate this problem, thresholding is used to cut off the noise which is lower than the given value (Th_{high}). Besides, this can reduce the total computation of COG. The resultant coordinate (v_{COG}) is examined whether it actually lies in the laser line regions. The coordinate is considered as proper one if the intensity at the coordinate is higher than another threshold (Th_{low}).

Thinning process is illustrated in Fig. 5. The upper left one shows the laser line image and the lower left shows the obtained center lines. The right one shows the intensity profile in the vertical direction. Two thresholds are defined and the coordinate is computed from the values above the high threshold.

Above process is for the vertical direction only. Depending on the material and reflection condition of the surface, the obtained center lines often have rough surfaces. The surface profile shows the difference of several pixels between adjacent coordinates in the horizontal direction. In most cases, the smooth profile is expected. To this aim, the averaging window is used. The coordinate is computed in an averaging window of which size is N by considering the closest $(N - 1)/2$ neighbors of each horizontal position u . Fig. 6 depicts the smoothing process whose window size is 3.

The size of window affects the characteristic of the profile measurement. Smaller window gives a bumpy surface, but the localization of the abrupt depth is better. On the other hand, larger window gives a smooth surface, but it is hard to localize the gap or step. Fig. 7 shows the averaging results when the sizes of window are 3, 11, and 21. We can get the best result when $N = 3$, because the gap

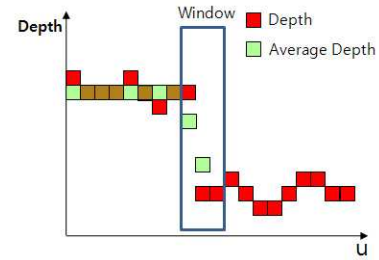


Fig. 6. Averaging window for smoothing

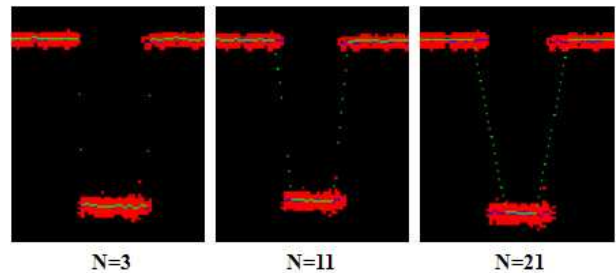


Fig. 7. Averaging results with different window sizes

and seam detection is relatively important in the welding application.

Finally, the camera calibration is needed to convert the profile points in image plane to the points in real Cartesian coordinates. Because the profile points lie in the triangular light plane projected by the laser, the 3D coordinate of those can be obtained uniquely. The relation between two coordinates is represented as direct linear transformation (DLT) (Abdel-Aziz et al. (1971)) and its coefficients can be determined by corresponding points. To give the corresponding points in each space, the calibration block having stair steps is used (Zhang (1998)). The Harris corner detector helps the selection of the corresponding points.

The calibration procedure should be performed with each configuration for the sensor to operate at different working distances. The desired accuracy is $200 \mu m$, and thus the camera should have about 20mm field of view in depth direction. The working distances can vary from 100mm to 300mm, and 5 uniformly separated configurations are considered. The relative angle between the camera and the laser diode and the lens parameters are adjusted appropriately. The relative angle is determined so that the nominal profile lies at the middle of the image plane. The zoom factor is selected first in order to view almost same physical depth range and the focus is determined to get the clearest laser image. After the calibration procedures of each configuration are performed, all parameters are stored in memory. The configuration is selected automatically according to the average depth of the last profile scanning. To avoid oscillatory changes between two neighboring configuration, the hysteresis is used near the boundaries.

3.3 Gap and Seam Extraction

The gap and seam extractions are critical operations in the robot laser welding, because the welding quality is influenced by them. The shape shown in Fig. 7 is an example with a gap and we want to find the width of

a gap. The seam detection can be varied according to the joints: butt, lap, V-groove, fillet joints and so on. However, the principle is the same for all cases. In this research, the butt joint is considered because it is common in automobile laser welding and the detection of it is relatively difficult. In both gap and seam detections, an elementary task is to recognize the difference in depth profile. This is similar to the edge detection in the image processing if the depth is corresponding to the intensity.

The simplest method for the edge detection is to find the depth differences between adjacent positions. Generally, this is done by applying a mask to the depth profile. Finally, the maximum (minimum) position is extracted as a rising (falling) edge. Among numerous edge detectors, Canny edge detector is most popular because it gives the best results in many applications (Canny (1986)). The edge is found so that the three criteria, i.e., good detection, good localization and uniqueness of response, are optimized. Generally speaking, the mask which resembles the shape of the edge itself is the optimal filter. For the step edge in the noise free environment, difference of boxes is the optimal mask. For the step edge in the noisy environment, it is hard to find the extreme position with difference of boxes because several peaks occur. In this case, another type of mask is the optimal and the difference of Gaussian (DOG) is used to approximate it.

In this research, the DOG operator is used to find the step edge. To estimate the gap, the distance between rising and falling edges is calculated. For the seam detection, the edge detection method can be also utilized. The matched filter is applied to the profile data according to the shape of the joint. Theoretically, it is impossible to localize the seam of a butt joint. However, the cutting edges of the joints hardly match each other and even diffused reflections occur at the joint. In addition, the jig cannot fix the joints perfectly. In Fig. 8, a sample image of the butt joint is given. Minute difference is found at the seam location and the thickness of the laser line at this location is smaller than in other regions. Therefore, the recognition of the narrow laser line as well as the edge detection is used for the seam detection of a butt joint. The detected seam location is also indicated in Fig. 8.

4. SENSOR GUIDED CONTROL SCHEME

Previously, the robot trajectories are given by human operator. The seam locations are taught with the operation panel. In this research, the seam locations are not given prior and the laser-stripe sensor guides the robot to the seam line.

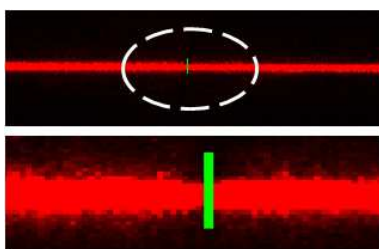


Fig. 8. Seam detection of a butt joint

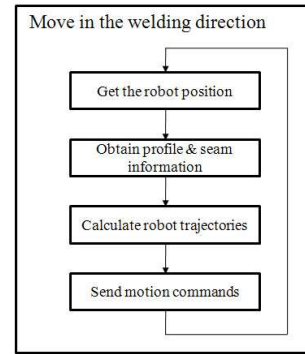


Fig. 9. Control architecture

For the experiment, the robot just moves in the welding direction following a straight line. The control architecture to track the seam line is done in the inner loop shown in Fig. 9. The robot position and the profile and seam information are obtained. From these, the robot trajectories are generated. After all, the motion commands are sent to the robot controller. The control is synchronized with the operation of the stripe sensor and the control interval is about 70 ms. After the motion commands are transferred to the robot controller, it takes tens of milliseconds to track the given position perfectly. The control method is needed to compensate this delay.

The sensor guided control methods were proposed by several researchers (Graaf et al. (2005); Zhou et al. (2006)). The operating frequency of the sensor, the look-ahead-distance, and the synchronization affect the tracking performance. In this study, a predictive control scheme similar to the trajectory-based control (Graaf et al. (2005)) is used. Fig. 10 shows this control scheme.

The sensor is attached away from the welding position by the look-ahead-distance. The sensor moves in front of the welding head and the seam locations are captured in advance. The seam locations are obtained at each horizontal interval and stored in the seam location buffer. The current velocity is updated by averaging previous velocities measured at each sampling interval. The current velocity of the robot is measured and the average velocity is updated as:

$$v_{avr}(k) = \alpha v_{current}(k) + (1 - \alpha)v_{avr}(k - 1) \quad (2)$$

where α is a constant with $0 \leq \alpha \leq 1$.

With the average velocity of the robot, the predicted position of the robot in the welding direction is estimated as:

$$x_{pred}(k) = x_{current}(k) + kv_{avr}(k) \quad (3)$$

where k is a prediction step in the unit of the control interval. Note that the predicted position in the welding

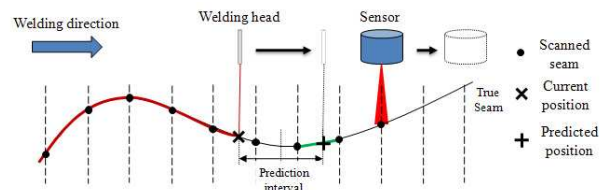


Fig. 10. Sensor guided control scheme

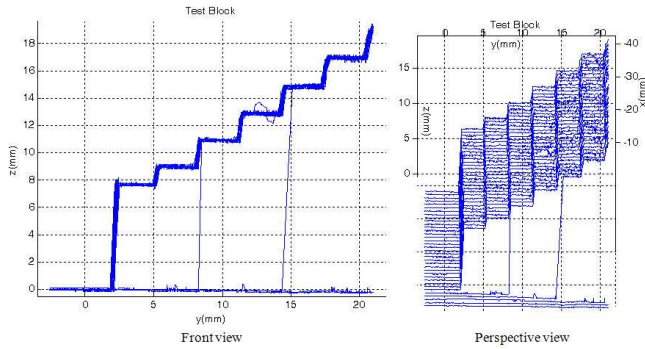


Fig. 11. Profile measurement of the calibration block

direction should be located before the last seam location in the welding direction. Finally, the seam location (or deviation) at the predicted position is computed. The linear interpolation is used to find the seam location that is not in the seam location buffer. A proper filtering can be considered to prevent unstable motion behavior.

The trajectory-based control has several advantages over the time-based methods which uses the sensor measurements directly within the time-based feedback loop. The seam locations are stored independent of time and the seam trajectory can be modified or removed if there exists unreliable reading. This also reduces the performance dependency on the sampling time and the look-ahead-distance. With this scheme, the tracking control of the seam location is achieved.

5. EXPERIMENTS

In this section, the measurement accuracy is evaluated from several experiments. The experiments include the profile measurement, the gap measurement, and the seam tracking test.

First, the profile of the calibration block has been measured. The calibration block is designed to have stair steps and used to calibrate the laser-stripe sensor. The exact dimension is known and the measurement accuracy can be evaluated. The robot moves at the velocity of 0.6 m/min and the profile measurement is done at every 1 mm . The result is shown in Fig. 11. The measurement accuracy in depth is about $120 \mu\text{m}$.

Several objects including a calibration block, a lap joint and an object with holes, has been scanned using the robot system. The sample objects and their profiles are shown in Fig. 12. It is shown that the profiles have quite smooth surfaces. However, there exists the region of which profile data cannot be obtained. This is because the laser diode declines and some profiles in the shaded region cannot be processed. The interpolation technique can be used to fill the absent profiles in this case.

Second, the gap measurement experiment has been performed. The specimen was made for this test and it has the various gaps of which sizes are varying from 0.2 mm to 1.0 mm . The specimen is shown in Fig. 13.

The results of the gap measurement are shown in Fig. 14. The experiment has been performed with different welding speeds (0.6 m/min and 3.0 m/min). The root

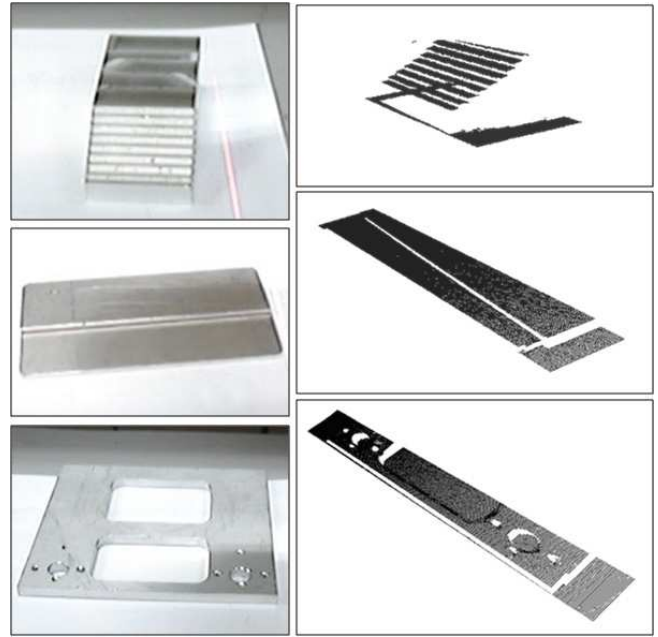


Fig. 12. Sample specimens and their profiles

mean squared errors (RMSE) of two cases are $48 \mu\text{m}$ and $35 \mu\text{m}$, respectively. The averaging window in depth plays an important role in the robust estimation. The accuracy of the gap measurement is better than that of the profile measurement because the horizontal resolution is higher than the vertical resolution.

Finally, the S-shaped seam tracking has been carried out. Fig. 15 shows the S-shaped butt joint and its dimension. Considering most shapes of joints in automobile parts are straight lines, the tracking of the S-shaped butt joint is a complex task. In this experiment, the true seam line is not given prior as mentioned earlier and the robot starts to follow a straight line. The seam line is scanned from the laser-stripe sensor and the trajectory of the robot is modified. The experiments were performed with different



Fig. 13. Specimen with various gap widths

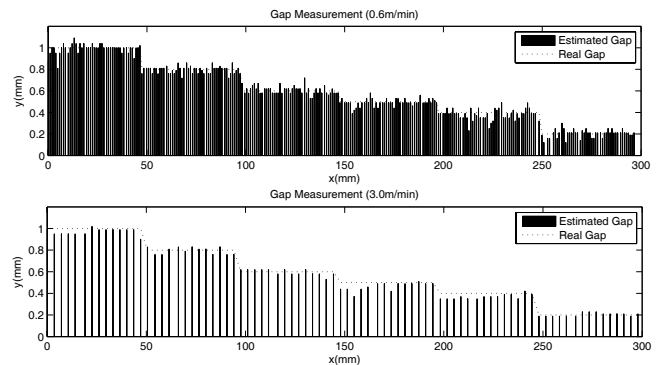


Fig. 14. Gap measurement

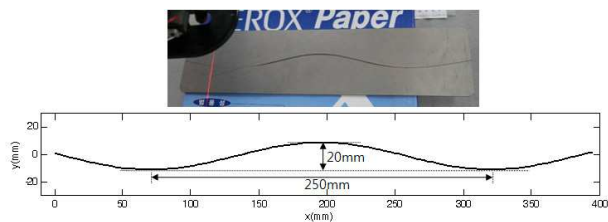


Fig. 15. S-shaped seam line and its dimension

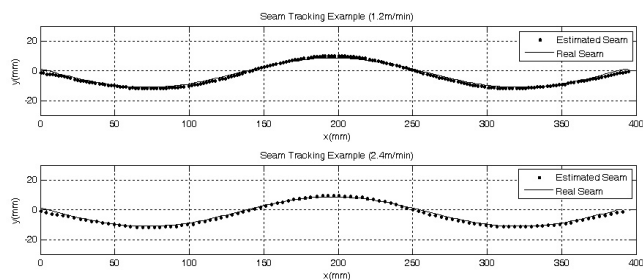


Fig. 16. Seam tracking results

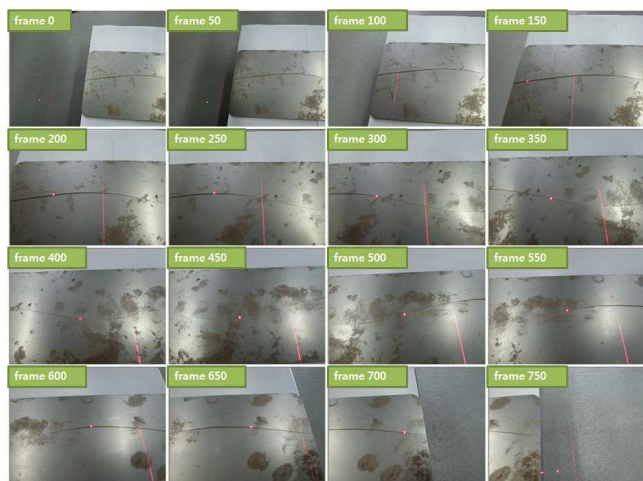


Fig. 17. Still images of S-shaped seam tracking

welding speeds (1.2 m/min and 2.4 m/min). The tracking results are shown in Fig. 16. The resulting accuracy of the seam locations is well within $200\ \mu\text{m}$. Fig. 17 shows the still images taken during the tracking of the S-shaped seam. The spot indicates the virtual welding position and it is found to track the seam locations with a good accuracy.

6. CONCLUSION

In this paper, the development of 3D laser welding robot system is represented. With the guide of the sensor, the robot can follow the seam of the welding part. Especially, a stripe-laser sensor is newly developed to be substituted for the commercial seam tracker. The sensor is designed to operate at different working distances. To measure the 3D profile data correctly, the thinning based on COG and the thresholding are implemented. For the robust estimation, the averaging methods are used as well. The detection of the gap and seam is achieved from the obtained depth profile. Finally, a simple prediction control scheme is used for the sensor guided robot control. The measurement and tracking accuracy are evaluated from various experiments.

For the future works, the interpolation technique to fill the absent region will be implemented. Also, to make the image processing procedures more efficient and more robust is important to enhance the tracking performance.

REFERENCES

- Abdel-Aziz, Y.I. and H.M. Karara (1971). Direct linear transformation from comparator coordinates into object space coordinates in close-range photogrammetry. In *Proc. the Symposium on Close-Range Photogrammetry*, pages 1–18, 1971.
- Canny, J. (1986). A computational approach to edge detection. *IEEE Trans. Pattern Anal. Mach. Intell.*, 8 (6):679–698, 1986.
- Forest, J. and J. Salvi (2002). A review of laser scanning three-dimensional digitisers. In *Proc. IEEE Conf. on Intelligent Robots and Systems (IROS'02)*, pages 73–78, Lausanne, Switzerland, October 2002.
- Graaf, M.W., R.G.K.M. Aarts, J. Meijer and J.B. Jonker (2005). Robot-sensor synchronization for real-time seam-tracking in robotic laser welding. In *Proc. WLT-Conf. on Lasers in Manufacturing*, pages 419–424, Munich, Germany, June 2005.
- Haug, K. and G. Pritschow (1998). Robust laser-stripe sensor for automated weld-seam-tracking in the ship-building industry. In *Proc. Conf. of the IEEE Industrial Electronics Society (IECON'98)*, pages 1236–1241, Aachen, Germany, August 1998.
- Zhang, Z. (1998). A flexible new technique for camera calibration, 1998. URL <http://research.microsoft.com/%7Ezhang/calib/>.
- Zhou, L., T. Lin and S.B. Chen (2006). Autonomous acquisition of seam coordinates for arc welding robot based on visual servoing. *Journal of Intelligent and Robotic Systems*, 47(3):239–255.